

Photoresponse of GaN:ZnO Electrode on FTO under Visible Light Irradiation

Hiroshi Hashiguchi,[1] Kazuhiko Maeda,[1,3] Ryu Abe,[2] Akio Ishikawa,[1] Jun Kubota,[1] and Kazunari Domen*[1]

[1]Department of Chemical System Engineering, The University of Tokyo, 7-3-1 Hongo, Bunkyo-ku, Tokyo 113-8656

[2]Catalysis Research Center, Hokkaido University, North 21, West 10, Sapporo 001-0021

[3]Research Fellow of the Japan Society for the Promotion of Science (JSPS), Chiyoda-ku, Tokyo 102-8471

Received August 6, 2008; E-mail: domen@chemsys.t.u-tokyo.ac.jp

The photoelectrochemical properties of a GaN:ZnO solid solution coated as an electrode on conductive glass are investigated through measurement of voltammograms and current–time curves. The highest photocurrent was achieved by a GaN:ZnO sample with relatively high zinc concentration (Zn/Ga = 0.42) and small particle size, presumably due to more efficient electron transfer through the porous electrode. The electrode exhibits anodic photocurrent under visible light, indicating functionality as an n-type semiconductor electrode. The estimated band-gap position of GaN:ZnO is located at satisfactory potential for water splitting. The bottom of the conduction band is similar to that for GaN, while the top of the valence band is substantially higher than that of either GaN or ZnO. The evolution of H_2 and O_2 is confirmed during photoelectrolysis at +0.5 V vs. Ag/AgCl. The efficiency of photoelectrolysis is found to decrease with irradiation time due to degradation of the electrode.

The photocatalytic and photoelectrochemical properties of semiconductor materials have been studied extensively in attempts to realize industrially practical solar energy conversion by water splitting under natural light. Many materials activated by ultraviolet (UV) light have been developed to date as powder photocatalysts for photocatalytic system or photoelectrodes for photoelectrochemical cells.[1–6] However, the achievement of efficient visible-light-driven photocatalysis is more important in terms of solar energy conversion. Only a few photoelectrode materials, such as WO_3 and $BiVO_4$, are able to decompose water to form O_2 under visible irradiation, and such materials require an externally applied potential to satisfy the thermodynamics determined by the band-gap position.[7–9] Reproducible overall water splitting under visible light has been achieved in a small number of cases involving one-step photocatalysis and Z-scheme systems.[10–13] Photoelectrodes prepared from photocatalytic materials activated by visible light are promising with respect to the development of photochemical solar cells. However, while such materials are stable and have a suitable band gap for overall water splitting, the fabrication of photoelectrodes has proven difficult due to problems encountered in processing the powder samples.

A solid solution of GaN and ZnO (GaN:ZnO) loaded with nanoparticulate RuO_2 or Rh–Cr_2O_3 as a cocatalyst has been demonstrated to decompose water under visible light by a one-step photoexcitation process.[10] The zinc content of GaN:ZnO, which is prepared by the nitridation of a mixture of GaN and ZnO under NH_3, can be adjusted by appropriate selection of the temperature and duration of nitridation. The band-gap energy of this solid solution has been shown to decrease with increasing zinc concentration, from 3.4 eV at Zn/Ga = 0 to 2.6 eV at Zn/Ga = 0.22.[14] Density functional theory (DFT) calculations suggest that the level of the valence band is strongly influenced by p–d repulsion between the Zn 3d and N 2p orbitals in the valence band.[14] However, recent photoluminescence experiments indicate that the addition of zinc species results in the formation of doping bands within the original band gap of GaN.[15] Confirmation of the band-gap position of GaN:ZnO requires further detailed analysis of the electrochemical and photoelectrochemical properties of GaN:ZnO.

In the present study, the photoelectrochemical properties of GaN:ZnO coated as electrodes on fluorine-doped tin oxide (FTO) (transparent conductive glass) are investigated in detail. The band gap of GaN:ZnO is determined on the basis of the onset potential of photocurrent under visible irradiation at wavelengths longer than 400 nm. The effects of IrO_2, a cocatalyst for water oxidation, on photocurrent are also investigated.

Experimental

Preparation of GaN:ZnO/FTO Electrodes. A powder of the GaN:ZnO solid solution was prepared as reported previously.[14] Briefly, a mixture of Ga_2O_3 (99.9%; Kojundo Chemical Lab, Japan) and ZnO (95.0% from Wako Pure Chemical Industries, Japan; 99.0% from Kanto Chemical, Japan) powders (ca. 2 g) was heated under flowing NH_3 (250 $cm^3 min^{-1}$) at various temperatures (1123–1223 K) and for various durations in order to obtain materials with a range of zinc concentrations (Table 1). The GaN:ZnO electrode was fabricated by spreading a viscous slurry of the GaN:ZnO powder on an FTO slide (ca. 20 Ω; Asahi Glass, Japan). The substrates were cleaned in advance by ultrasonication

Published on the web March 12, 2009; doi:10.1246/bcsj.82.401

Table 1. EDX Compositions and BET Surface Areas of GaN:ZnO Powders

Nitridation time	Temperature /K	Zn/Ga atomic ratio	BET surface area/$m^2\,g^{-1}$
15 min	1223	0.42	9.9
1 h	1223	0.23	5.9
15 h	1123	0.17	6.0

in acetone and then distilled water. The slurry consisted of the as-prepared GaN:ZnO powder (0.2 g), water (400 μL), acetylacetone (20 μL), and a small amount of surfactant (Triton X-100, Aldrich, USA). After coating with the slurry to achieve an electrode area of $1 \times 4\,cm^2$, the slide was heated at 623 K in air for 1 h in order to remove organic solvent and surfactant and to enhance the attachment of particles to the substrate. 4 mg of powders were attached to the $1 \times 4\,cm^2$ FTO glass. The GaN:ZnO electrode thus fabricated was characterized by X-ray diffraction (XRD; RINT Ultima III, Rigaku, Japan), UV–visible diffuse reflectance spectroscopy (UV–vis DRS; V-560, Jasco, Japan), field-emission scanning electron microscopy (FE-SEM; S-4700, Hitachi, Japan), and energy-dispersive X-ray spectroscopy (EDX; EMAX 7000, Horiba, Japan). The Brunauer–Emmett–Teller (BET) surface area was measured at liquid nitrogen temperature (SA-3100, Beckman Coulter, USA).

Some of the GaN:ZnO electrodes were modified by adding $Zn(NO_3)_2$ to improve electron transfer within the porous electrode.[16,17] Modification was performed by applying 20 μL of an aqueous 0.1 M $Zn(NO_3)_2 \cdot 6H_2O$ (>99.0%; Kanto Chemical) solution onto the electrode using a pipette and then drying the electrode at ambient temperature. This process was repeated 3 times, and the electrode was finally heated under NH_3 flow ($100\,cm^3\,min^{-1}$) at 773 K for 1 h.

Another set of GaN:ZnO electrodes was loaded with IrO_2 as a cocatalyst by impregnation with an aqueous solution of $Na_2[IrCl_6] \cdot 6H_2O$ (>97.0%; Kanto Chemical). Impregnation was performed by applying a small amount of $Na_2[IrCl_6]$ aqueous solution onto the GaN:ZnO electrode using a pipette. The sample was dried at ambient temperature and then heated at 623 K in air for 1 h to convert the Ir species to IrO_2.

Photoelectrochemical Measurements. Current–voltage and current–time curves were measured using a conventional Pyrex electrochemical cell equipped with a planar window. The single-vessel electrochemical cell consisted of a prepared electrode, a platinum wire as a counter electrode (1 mm in diameter, 15 mm in length), and an Ag/AgCl reference electrode. The cell was filled with an aqueous solution of either 0.1 M NaI and 0.1 mM I_2, or 0.5 M Na_2SO_4, and the pH of the solution was 6.7 for NaI/I_2. The pH of solution of Na_2SO_4 was adjusted to 4.5 by adding H_2SO_4, because the photocurrent was maximum at pH 4.5. The GaN:ZnO photocatalysts with Rh–Cr oxide cocatalyst also shows the best performance at pH of 4.5.[18] The electrolyte was saturated with argon prior to electrochemical measurements, and the potential of the electrode was controlled by a potentiostat (HZ-5000, Hokuto Denko; SDPS-501C, Syrinx). Irradiation was performed through the conducting glass using a 300 W Xe lamp with a cold mirror and cutoff filters (Hoya) as necessary. It should be noted that the FTO glass did not show photoresponse in the solutions. The evolved gases were determined with gas chromatography (Shimadzu GC-8A, MS-5A, TCD, Ar carrier) which was directly connected to the cell. The incident photon-to-photocurrent efficiency of the photoelectrode was examined by a monochromatic light source with a band-pass filter at 420 nm with band-width (full-width at half-maximum) of 10 nm (Asahi Spectra). The energy of irradiation was measured by a calibrated Si photodiode (Hamamatsu) which had a detection area of $1.00\,cm^2$. It should be noted that the FTO substrate showed no photoresponse itself in the solutions.

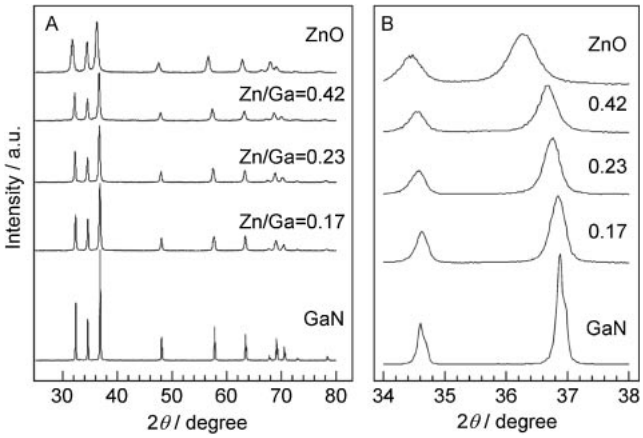

Figure 1. (A) XRD patterns of GaN:ZnO powders. (B) Detailed pattern in a 2θ range of 34–38°. Atomic ratios estimated by EDX are shown. Patterns for pure GaN and ZnO are shown for reference.

Results and Discussion

Characterization of GaN:ZnO Powder. The zinc concentration in GaN:ZnO is strongly influenced by the nitridation conditions, which affect ZnO reduction and subsequent zinc volatilization under a reductive atmosphere.[14] The Zn/Ga ratio was determined from the EDX results. Nitridation at 1123 K for periods of 5–30 h affords GaN:ZnO powders with relatively low Zn/Ga ratios (0.05–0.22), while nitridation for less than 5 h yields powders containing ZnO and $ZnGa_2O_4$ as impurity phases.[14] GaN:ZnO samples with zinc concentrations of Zn/Ga = 0.23 and 0.42 were successfully prepared in the present study by nitriding a mixture of Ga_2O_3 and ZnO with a Zn/Ga ratio of 1 at 1223 K for 15 min or 1 h, respectively. A sample of GaN:ZnO nitrided at 1123 K for 15 h under NH_3 flow was also prepared in the present study, as the powder afforded has been shown in previous work to exhibit the highest photocatalytic activity for water decomposition among all samples prepared at 1123 K.[14]

XRD patterns of the prepared GaN:ZnO powders, as well as GaN, and ZnO as starting materials, are shown in Figure 1. Nitridation at higher temperature (1223 K) and for shorter periods (15 min or 1 h) led to higher zinc concentrations in the present samples (Table 1). The diffraction patterns for all of the present samples indicate the presence of a single wurtzite phase similar to that of GaN and ZnO, without impurity phases. Rapid crystallization by nitridation at higher temperatures and for shorter periods thus affords GaN:ZnO with a single wurtzite phase and relatively high zinc concentration (Zn/Ga = 0.42).

Figure 2 shows the UV–vis diffuse reflectance spectra for the GaN:ZnO samples. The absorption edges of the present samples occur at substantially longer wavelengths than for GaN and ZnO, and the absorption edge shifts to longer wavelengths with increasing zinc concentration, consistent with the literature.[14] The band-gap energies of GaN:ZnO at zinc concen-

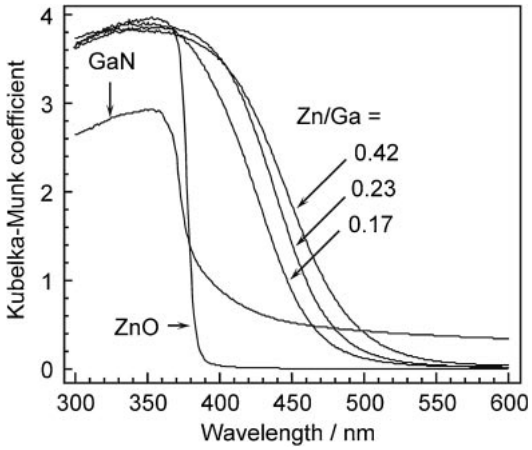

Figure 2. UV–vis DR spectra of GaN:ZnO powders. Atomic ratios estimated by EDX are shown. Spectra for pure GaN and ZnO are shown for reference.

trations of Zn/Ga = 0.17, 0.23, and 0.42 are estimated to be ca. 2.8, 2.6, and 2.5 eV, respectively, based on the diffuse reflectance spectra.[14,18,19]

Photoelectrochemical Properties of GaN:ZnO Electrodes in NaI/I_2 Solution. The nitridation conditions applied in the synthesis of GaN:ZnO affect several properties of the material obtained, including the zinc concentration, surface area, and band-gap energy. In the present study, three GaN:ZnO samples prepared under different conditions were evaluated in terms of photoelectrochemical properties. Cyclic voltammograms of the GaN:ZnO electrodes were initially measured in 0.5 M Na_2SO_4 solution in order to select suitable samples for photoelectrochemical measurements. All samples exhibited low photocurrent of 1–3 μA cm^{-2} at 0.5 V vs. Ag/AgCl. Electron transfer within the porous electrode was improved by modification with $Zn(NO_3)_2$ solution followed by heat treatment under NH_3 flow.[16–18] A mixed aqueous solution (pH 6.7) of 0.1 M NaI and 0.1 mM I_2 was employed as the electrolyte to enhance photocurrent and maintain electrode stability. Zinc treatment was found to enhance the photocurrent by up to 10 times. It was speculated that the $Zn(NO_3)_2$ species was reduced by flow of NH_3 in the heat treatment but re-oxidized by air. The presence of Zn metal was unlike in the aqueous solution with potential sweeping, and some Zn^{2+} (ZnO) species remained between GaN:ZnO particles.

Current–voltage curves of the zinc-treated GaN:ZnO electrodes under UV irradiation are shown in Figure 3 along with the curves for a GaN electrode. Anodic photocurrent was clearly observed for the electrodes with Zn/Ga ratios of 0.23 and 0.42. The electrode with Zn/Ga = 0.42 exhibited the highest performance of the electrodes tested, achieving an anodic photocurrent of 400 μA cm^{-2} at 0.3 V vs. Ag/AgCl. The appearance of anodic photocurrent indicates that the GaN:ZnO functioned as an n-type semiconductor. GaN and GaN:ZnO with a Zn/Ga ratio of 0.13 exhibited a small photoresponse over the entire range of potential. The small cathodic current under irradiation appeared with irradiation of longer wavelength light than the band gap, indicative of a thermal effect.

GaN:ZnO with a Ga/Zn ratio of 0.17 was found in a previous study to exhibit the highest photocatalytic activity for

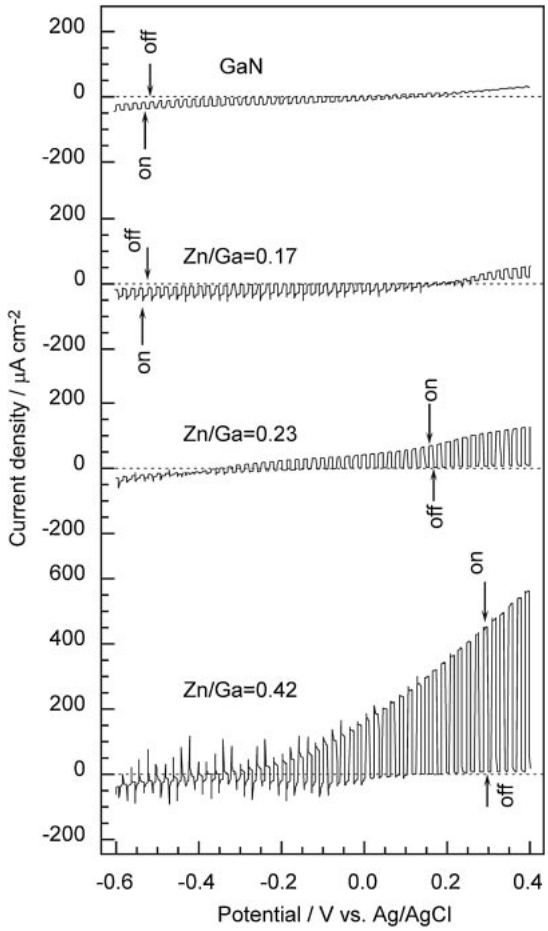

Figure 3. Current–voltage curves for GaN:ZnO electrodes under intermittent UV irradiation (>300 nm) in a mixed aqueous solution of 0.1 M NaI and 0.1 mM I_2 (pH 6.7). Sweep rate was 0.5 mV s^{-1}.

overall water splitting among the compositions tested as powder photocatalysts.[14] In the previous case, the material was obtained by nitridation at 1123 K for 15 h. In the present study however the photoelectrode with composition of Zn/Ga = 0.42 achieved substantially higher performance than the compositions with smaller Zn/Ga ratios. Figure 4 shows SEM images of the present GaN:ZnO samples. The average particle size of the Zn/Ga = 0.42 sample is approximately 200 nm, half that of the Zn/Ga = 0.17 and 0.23 samples (ca. 400 nm). These observations are consistent with BET measurements (Table 1), which show that the Zn/Ga = 0.42 sample has the highest surface area of the present samples. For powder catalysis, high crystallinity is generally required in order to inhibit the recombination of electrons and holes. For the electrode film on the other hand, smaller particles generally result in the formation of denser powders, improving electron transfers between particles. In the electrochemical GaN:ZnO system, electron transfer within the porous electrode is therefore considered to be more important than crystallinity in terms of the transport of electrons to the FTO through each particle. Short nitridation (15 min) afforded a GaN:ZnO sample with high zinc concentration (Zn/Ga = 0.42) but with lower crystallinity than that of samples with lower Zn/Ga ratios. In

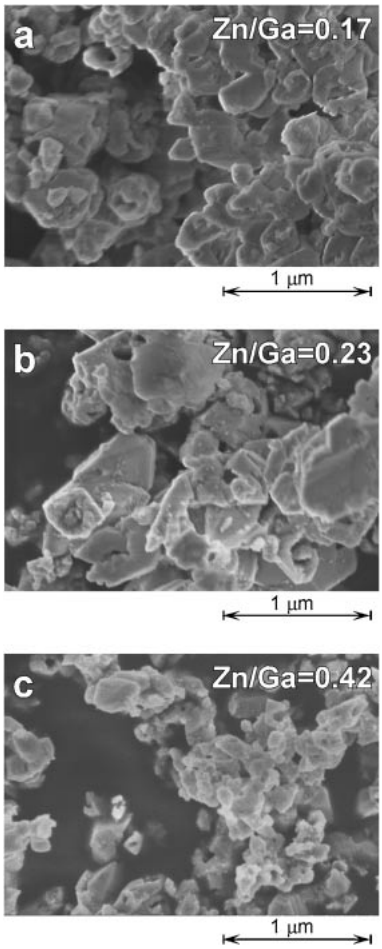

Figure 4. SEM images of GaN:ZnO powders with Zn/Ga ratios of (a) 0.17, (b) 0.23, and (c) 0.42.

the photoelectrode system, the electric conductivity between the particles and between the particle and the substrate is an absolute requirement for performance, so the optimized Zn/Ga ratio was different from that for photocatalysis. Therefore, the difference in performance between the electrochemical and photocatalytic GaN:ZnO systems appears to be due to the differing effects of particle size and crystallinity in the two systems.

The GaN:ZnO electrode with Zn/Ga ratio of 0.42 also exhibited strong photoresponse in a mixed solution of 0.1 M NaI and 0.1 mM I_2 after zinc treatment. The Zn/Ga = 0.42 composition was therefore used to evaluate the photoelectrochemical properties (e.g., band-gap position) of GaN:ZnO in 0.5 M Na_2SO_4. As it was expected that the presence of zinc species on the surface of the GaN:ZnO samples would make it difficult to evaluate the band-gap position of GaN:ZnO, even though zinc treatment was found to enhance the photocurrent of the electrode, photoelectrochemical measurements were carried out using GaN:ZnO electrodes without zinc treatment.

Band-Gap Position of GaN:ZnO Solid Solution. To establish the band-gap position of GaN:ZnO (without zinc treatment), the onset potential for anodic photocurrent was measured in 0.5 M Na_2SO_4 solution, adjusted to pH 4.5 using H_2SO_4, under irradiation at visible wavelengths (>420 nm). Figure 5 shows the current–voltage curve for the GaN:ZnO

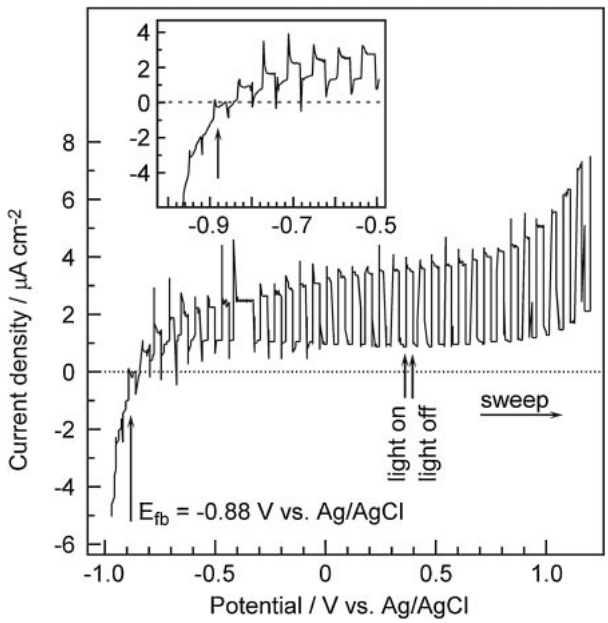

Figure 5. Current–voltage curve for GaN:ZnO electrode under intermittent visible irradiation (>420 nm) in 0.5 M Na_2SO_4 (pH 4.5). Sweep rate was 0.5 mV s^{-1}.

electrode with Zn/Ga = 0.42 at a scanning potential of −1.0 to 1.2 V. The anodic photocurrent appears at −0.88 V vs. Ag/AgCl (−0.68 V vs. NHE). The flat-band potential (E_{FB}), which is equal to the Fermi level (E_F) of the GaN:ZnO electrode, is equivalent to the onset potential of photocurrent. Thus, E_{FB} was estimated to be −0.68 V vs. NHE including the error of ±0.1 V. The bottom of the conduction band (E_{CB}) is estimated to be located at ca. −0.78 V vs. NHE based on the energy difference between E_F and E_{CB} (assumed to be ca. 0.1 V),[20,21] and the band-gap energy (E_{BG}) is estimated to be approximately 2.5 eV from the UV–vis DRS results (Figure 2). The top of the valence band (E_{VB}) is estimated to lie at +1.72 V vs. NHE. The band-gap position of GaN:ZnO with composition of Zn/Ga = 0.42 is illustrated in Figure 6. For comparison, the band-gap position of GaN, which varies with the pH of the solution,[21–23] is also shown. The E_{CB} values for GaN and GaN:ZnO are similar, which is reasonable considering that the conduction bands of both materials are populated by Ga 4s and 4p orbitals.

In the case of tantalum-based materials (Ta_3N_5, TaON, and Ta_2O_5), in which the conduction band is populated by Ta 5d orbitals, E_{CB} are similar in the range −0.3 to −0.5 V (vs. NHE at pH 0), while E_{BG} and E_{VB} increase in the order Ta_3N_5 < TaON < Ta_2O_5.[23] DFT calculations indicate that the valence bands for Ta_3N_5, TaON, and Ta_2O_5 consist mainly of N2p, O2p + N2p, and O2p orbitals, respectively, suggesting that the changes in orbitals lead to changes in E_{VB}. In the case of GaN:ZnO, the band-gap energy increases with decreasing zinc and oxygen concentration, indicating that the presence of both elements affects E_{VB}. The E_{CB} and E_{VB} values for ZnO are however different from those for GaN:ZnO, as shown in Figure 6.[25] The similarity of E_{CB} values for GaN:ZnO and GaN suggests that the main band structure of GaN:ZnO is the same as that of GaN. The mechanism of the shift of E_{VB} to higher

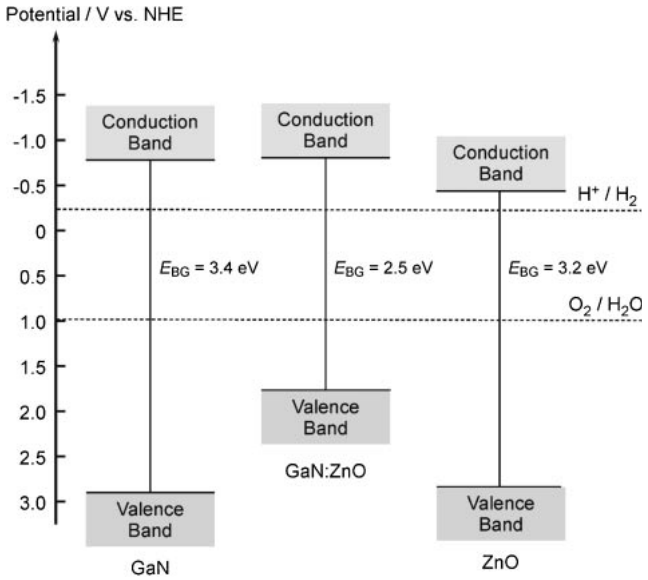

Figure 6. Schematic illustration of band structure of GaN and GaN:ZnO at pH 4.5.

potential energy with increasing zinc and oxygen concentration is therefore somewhat complex, and further investigations will be required for clarification. Photoluminescence analyses are currently being undertaken as part of such an investigation.

GaN:ZnO with a Zn/Ga ratio of 0.42 exhibits a conduction band minimum (E_{CB}) similar to that of GaN, while the top of the valence band (E_{VB}) occurs at much higher potential than that of either GaN or ZnO. The estimated band-gap position of GaN:ZnO is suitable for overall water decomposition, consistent with the results for photocatalysis. Photocurrent onset is at -0.68 V vs. NHE, which is higher than the potential of H_2/H^+ (-0.27 V) at pH 4.5, indicating that the GaN:ZnO electrode is possibly applicable in a photovoltaic cell for overall water splitting.

Effect of IrO_2 on Photocurrent of GaN:ZnO Electrodes. The GaN:ZnO electrode functions as an n-type electrode, catalyzing the oxidation of water to O_2 under visible light. IrO_2 is also a known catalyst for the oxidation of water and has been used in both electrochemistry and photocatalysis.[26–31] Figure 7 shows how loading the GaN:ZnO electrode with IrO_2 as a cocatalyst affects the photocurrent of the electrode in 0.5 M Na_2SO_4 under irradiation at visible wavelengths (>420 nm). Loading with IrO_2 results in a marked increase in photocurrent over that of the original electrode, particularly in the potential range of 0.3–1.2 V vs. Ag/AgCl. The effect of IrO_2 on photocurrent is much less remarkable in the -0.9 to 0.3 V vs. Ag/AgCl range, apparently due to suppressed electron transfer and the inherently high electrical resistance of the GaN:ZnO powder. It should be noted that the dark current of the IrO_2-loaded electrode increased above 1.0 V vs. Ag/AgCl. This current originated from O_2 evolution on IrO_2 in the dark which was deposited on FTO directly. The FTO is less active for O_2 evolution as seen in Figure 7A, but IrO_2 loading increased the O_2 evolution current. The IrO_2 deposited on GaN:ZnO was not expected to evolve O_2 in the dark, because GaN:ZnO is an n-type semiconductor and not conductive in the dark. The

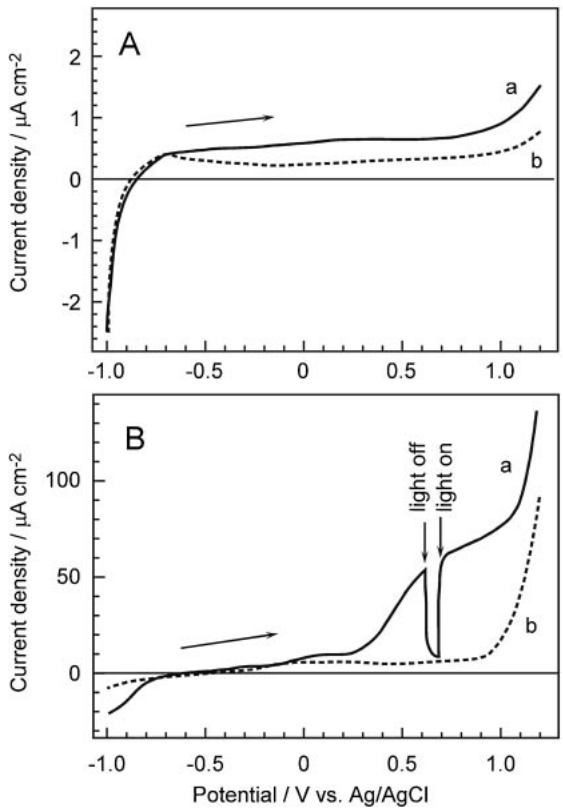

Figure 7. Schematic current–voltage curves for (A) GaN:ZnO and (B) GaN:ZnO loaded with IrO_2 (10 wt %) under (a) visible irradiation (>420 nm) and (b) darkness. Sweep rate was 0.5 mV s^{-1}.

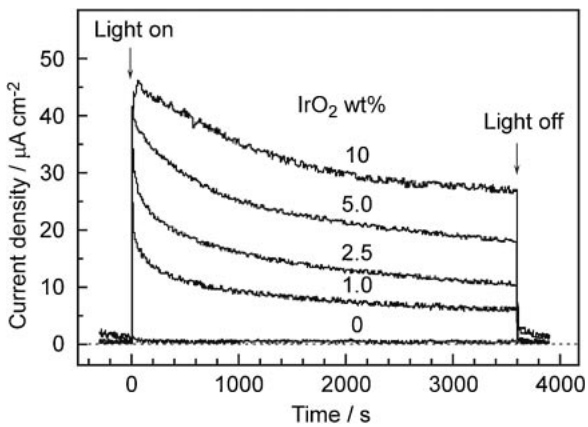

Figure 8. Time course of photocurrent under visible irradiation (>420 nm) for IrO_2-loaded GaN:ZnO electrodes at 0.5 V vs. AgCl (pH 4.5).

dependence of photocurrent enhancement on the amount of IrO_2 loading is shown in Figure 8, where the potential was set to 0.5 V vs. Ag/AgCl (0.7 V vs. NHE) because of small photocurrent at -0.27 V vs. NHE (reversible potential for H_2 evolution). Thus this potential was theoretically equivalent to the 0.97 V of bias voltage against the counter electrode which produces H_2. The photocurrent density was found to increase progressively with increasing IrO_2 content to a maximum at 10 wt % IrO_2.

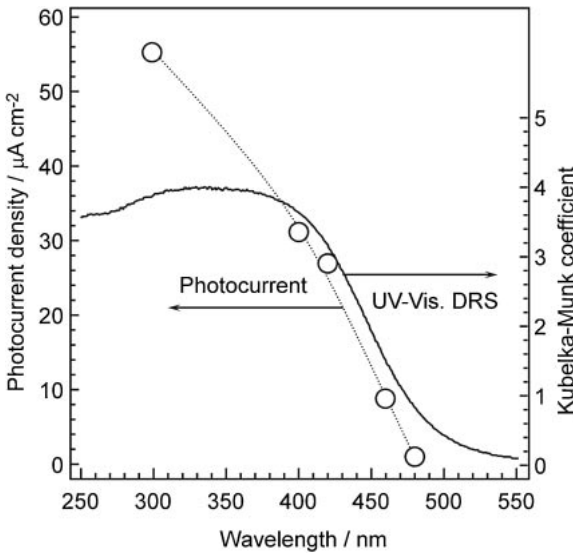

Figure 9. Dependence of photocurrent of IrO_2-loaded GaN:ZnO on irradiation wavelength (open circles). UV–vis DR spectrum is also shown (solid line). Photocurrent was measured at 0.5 V vs. Ag/AgCl after irradiation for 1 h.

The dependence of initial photocurrent on the cutoff wavelength of incident light is shown in Figure 9. These data were obtained by irradiating samples via appropriate cutoff filters for the wavelength shown (photon counts decrease with increasing wavelength). The UV–vis DR spectrum for the GaN:ZnO powder is also shown in the figure. No photocurrent was observed when the sample was irradiated at wavelengths longer than 480 nm, consistent with the absorption edge in the UV–vis DR spectrum (ca. 480 nm). These results indicate that the photocurrent generated by the GaN:ZnO electrode loaded with 10 wt % IrO_2 is due to band-gap excitation of GaN:ZnO. Surface loading with IrO_2 therefore appears to increase the efficiency of the oxidation reaction by enhancing the efficiency of photogenerated hole consumption.

The incident photon-to-photocurrent efficiency, IPCE, is defined as

$$\mathrm{IPCE}(\%) = \frac{ch}{e}\frac{i_{\mathrm{photo}}}{\lambda\Phi} \times 100 \quad (1)$$

where i_{photo}, λ, and Φ are photocurrent density ($\mathrm{A\,m^{-2}}$), wavelength (m), and flux of light ($\mathrm{W\,m^{-2}}$), c, h, and e are the speed of light, Planck constant, and the elementary electric charge. Using a monochromatic light source at 420 nm, photocurrent of 9.8 $\mu\mathrm{A\,cm^{-2}}$ was obtained for 10 wt % IrO_2-loaded GaN:ZnO in 0.5 M Na_2SO_4 solution, adjusted to pH 4.5 at 0.5 V vs. Ag/AgCl. The flux of light was estimated as 10.0 $\mathrm{mW\,cm^{-2}}$, which was much smaller than the Xe lamp for the other measurements. The IPCE for 10 wt % IrO_2-loaded GaN:ZnO at 0.5 V vs. Ag/AgCl was thus derived as 0.29%.

The current–time curve for the GaN:ZnO electrode loaded with 10 wt % IrO_2 is shown in Figure 10, as measured under visible irradiation at a steady applied potential (0.5 V vs. Ag/AgCl). Over the full irradiation period (23.5 h), 5.9 μmol of O_2 and 12.2 μmol of H_2 (ca, 24 μmol electrons) were evolved on the working and counter electrodes. N_2 gas (7.1 μmol) was also

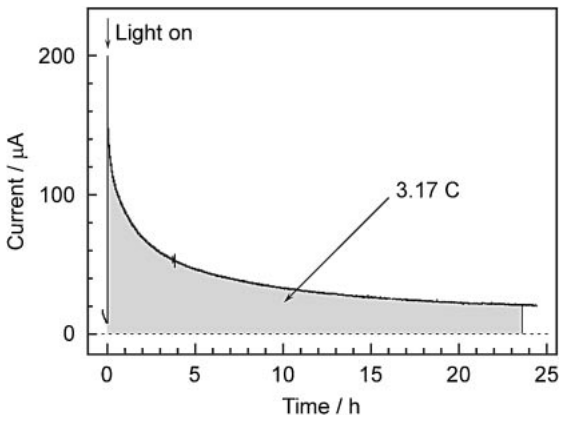

Figure 10. Time course of photocurrent of IrO_2-loaded GaN:ZnO photoelectrode under visible irradiation (420–550 nm) in 0.5 M Na_2SO_4 (pH 4.5) and at electrode potential of 0.5 V vs. Ag/AgCl. Evolution of 5.9 μmol O_2 and 12.2 μmol H_2 was detected after 23.5 h of reaction. Total charge of photoelectrolysis is estimated to be 3.17 C (23.5 h). Total current for $1 \times 4\,\mathrm{cm^2}$ area of electrode is shown (not current density).

detected, suggesting that the GaN:ZnO powder is decomposed in this photoelectrolysis reaction or that the experimental system was affected by small leaks. A total charge of 3.17 C (33 μmol electrons) is estimated by integration of the current–time curve, larger than the amount of electrons (ca. 24 μmol) calculated from the amount of evolved H_2. It is thought that the total amount of evolved H_2 and O_2 gases is lower due to back reaction on the platinum counter electrode before gas chromatography. The photocurrent of the GaN:ZnO electrode loaded with 10 wt % IrO_2 decreased through the experimental period (23.5 h). This decrease in photocurrent with irradiation time may be attributable to decomposition of the GaN:ZnO material, as observed for Ta_3N_5 on tantalum metal substrates[32] in 0.1 M K_2SO_4 and GaN on (0001) sapphire substrates[23] in 1 M H_2SO_4. Dye-sensitized cells,[17] which contain colloidal TiO_2 approximately 20 nm in size, are essentially stable due to the high mechanistic strength of the bond to the substrate.[16] Given the relatively large particle size (ca. 200 nm) of the present GaN:ZnO samples, it is believed that the mechanistic strength of the bond to the substrate is weak and a likely cause of electrode degradation.

The GaN:ZnO electrode loaded with IrO_2 thus functions as a visible-light-driven photoelectrode that decomposes water to O_2 at +0.5 V vs. Ag/AgCl under visible irradiation. H_2 evolution was also detected by gas chromatography. The efficiency of photoelectrolysis decreased as the reaction progressed due to degradation of the GaN:ZnO electrode, possibly by the liberation of GaN:ZnO particles from the substrate or decomposition of the GaN:ZnO material itself.

As mentioned in the previous section, the GaN:ZnO electrode shows photocurrent above −0.88 V vs. Ag/AgCl (−0.68 V vs. NHE). The pH of Na_2SO_4 solution was adjusted to 4.5, indicating that the potential of −0.68 V vs. NHE is lower than the hydrogen evolution −0.27 V vs. NHE. This fact suggests that the GaN:ZnO electrode can evolve O_2 by visible light irradiation even without applying potential. The amount

of evolved O_2 without applying potential was smaller than the detection limit in the present study, but the evolution of O_2 should occur the same as at +0.5 V.

Conclusion

Investigation of the photoelectrochemical properties of GaN:ZnO electrodes on FTO glass revealed that GaN:ZnO powder with a composition of $Zn/Ga = 0.42$ achieves the highest photocurrent of the compositions tested in a mixed solution of 0.1 M NaI and 0.1 mM I_2 under UV irradiation. The flat-band potential of GaN:ZnO was estimated, and the narrow band gap of GaN:ZnO compared to GaN was found to originate from the increase in the potential of the valence band. Modification of the GaN:ZnO electrode with IrO_2 was found to increase the photocurrent considerably in aqueous Na_2SO_4 solution. Photoelectrochemical water splitting over the GaN:ZnO/FTO electrode loaded with 10 wt% IrO_2 was successfully demonstrated at a bias potential of 0.5 V vs. Ag/AgCl, achieving stoichiometric H_2 and O_2 evolution. The electrode was found to become less active with progress of the reaction due to material degradation. Future studies will examine methods for improving the lifetime of the electrode.

This study was supported by the Development in a New Interdisciplinary Field Based on Nanotechnology and Materials Science program of the Ministry of Education, Culture, Sports, Science and Technology (MEXT) of Japan. It was also supported by Tokyo Metropolitan Collaboration of Regional Entities for the Advancement of Technological Excellence, Japan Science and Technology Agency (JST). One of the authors (K.M.) gratefully acknowledges the Japan Society for the Promotion of Science (JSPS) Fellowship.

References

1 A. Fujishima, K. Honda, *Nature* **1972**, *238*, 37.
2 K. Domen, A. Kudo, T. Onishi, *J. Catal.* **1986**, *102*, 92.
3 K. Domen, S. Naito, M. Soma, T. Onishi, K. Tamaru, *J. Chem. Soc., Chem. Commun.* **1980**, 543.
4 K. Domen, S. Naito, T. Onishi, K. Tamaru, *Chem. Phys. Lett.* **1982**, *92*, 433.
5 W. Erbs, J. Desilvestro, E. Borgarello, M. Grätzel, *J. Phys. Chem.* **1984**, *88*, 4001.
6 J. R. Darwent, A. Mills, *J. Chem. Soc., Faraday Trans. 2* **1982**, *78*, 359.
7 M. A. Butler, *J. Appl. Phys.* **1977**, *48*, 1914.
8 C. Santato, M. Odziemkowski, M. Ulmann, J. Augustynski, *J. Am. Chem. Soc.* **2001**, *123*, 10639.
9 K. Sayama, A. Nomura, Z. Zou, R. Abe, Y. Abe, H. Arakawa, *Chem. Commun.* **2003**, 2908.
10 K. Maeda, K. Teramura, D. Lu, T. Takata, N. Saito, Y. Inoue, K. Domen, *Nature* **2006**, *440*, 295.
11 Y. Lee, H. Terashima, Y. Shimodaira, K. Teramura, M. Hara, H. Kobayashi, K. Domen, M. Yashima, *J. Phys. Chem. C* **2007**, *111*, 1042.
12 K. Sayama, K. Mukasa, R. Abe, Y. Abe, H. Arakawa, *J. Photochem. Photobiol., A* **2002**, *148*, 71.
13 H. Kato, M. Hori, R. Konta, Y. Shimodaira, A. Kudo, *Chem. Lett.* **2004**, *33*, 1348.
14 K. Maeda, K. Teramura, T. Takata, M. Hara, N. Saito, K. Toda, Y. Inoue, H. Kobayashi, K. Domen, *J. Phys. Chem. B* **2005**, *109*, 20504.
15 T. Hirai, K. Maeda, M. Yoshida, J. Kubota, S. Ikeda, M. Matsumura, K. Domen, *J. Phys. Chem. C* **2007**, *111*, 18853.
16 R. Abe, T. Takata, H. Sugihara, K. Domen, *Chem. Lett.* **2005**, *34*, 1162.
17 M. K. Nazeeruddin, A. Kay, I. Rodicio, R. Humphyry-Baker, E. Mueller, P. Liska, N. Vlachopoulos, M. Grätzel, *J. Am. Chem. Soc.* **1993**, *115*, 6382.
18 K. Maeda, K. Teramura, H. Masuda, T. Takata, N. Saito, Y. Inoue, K. Domen, *J. Phys. Chem. B* **2006**, *110*, 13107.
19 K. Maeda, T. Takata, M. Hara, N. Saito, Y. Inoue, H. Kobayashi, K. Domen, *J. Am. Chem. Soc.* **2005**, *127*, 8286.
20 Y. Matsumoto, *J. Solid State Chem.* **1996**, *126*, 227.
21 S. S. Kocha, M. W. Peterson, D. J. Arent, J. M. Redwing, M. A. Tischler, J. A. Turner, *J. Electrochem. Soc.* **1995**, *142*, L238.
22 J. D. Beach, R. T. Collins, J. A. Turner, *J. Electrochem. Soc.* **2003**, *150*, A899.
23 I. M. Huygens, K. Strubbe, W. P. Gomes, *J. Electrochem. Soc.* **2000**, *147*, 1797.
24 W.-J. Chun, A. Ishikawa, H. Fujisawa, T. Takata, J. N. Kondo, M. Hara, M. Kawai, Y. Matsumoto, K. Domen, *J. Phys. Chem. B* **2003**, *107*, 1798.
25 H. Genscher, *J. Electrochem. Soc.* **1966**, *113*, 1174.
26 S. Trasatti, *Electrochim. Acta* **1984**, *29*, 1503.
27 A. Harriman, I. J. Pickering, J. M. Thomas, P. A. Christensen, *J. Chem. Soc., Faraday Trans. 1* **1988**, *84*, 2795.
28 A. Ishikawa, T. Takata, J. N. Kondo, M. Hara, H. Kobayashi, K. Domen, *J. Am. Chem. Soc.* **2002**, *124*, 13547.
29 A. Iwase, H. Kato, A. Kudo, *Chem. Lett.* **2005**, *34*, 946.
30 A. Kasahara, K. Nukumizu, G. Hitoki, T. Takata, J. N. Kondo, M. Hara, H. Kobayashi, K. Domen, *J. Phys. Chem. A* **2002**, *106*, 6750.
31 M. Hara, C. C. Waraksa, J. T. Lean, B. A. Lewis, T. E. Mallouk, *J. Phys. Chem. A* **2000**, *104*, 5275.
32 A. Ishikawa, T. Takata, J. N. Kondo, M. Hara, K. Domen, *J. Phys. Chem. B* **2004**, *108*, 11049.